1   **Title:** *Evolution of the genetic architecture of local adaptations under genetic rescue is*

2   *determined by mutational load and polygenicity*

3

4   **Running title:** *Local adaptations under genetic rescue*

5

6   **Authors**: Yulin Zhang[1,2,*], Aaron J. Stern[2,*,+], Rasmus Nielsen[3,4,5+]

7

8   [1]School of Life Sciences, Sun Yat-sen University, Guangzhou, Guangdong, P.R.China

9   [2]Graduate Group in Computational Biology, UC Berkeley, Berkeley, CA 94707, USA.

10   [3]Department of Integrative Biology, UC Berkeley, Berkeley, CA 94707, USA.

11   [4]Department of Statistics, UC Berkeley, Berkeley, CA 94707, USA.

12   [5]Natural History Museum of Denmark, University of Copenhagen, 1350 København K,

13   Denmark.

14

15   *Authors contributed equally

16   +Corresponding authors: AJS: ajstern@berkeley.edu, RN: rasmus_nielsen@berkeley.edu

17

18   **Abstract:**

19   Inbred populations often suffer from heightened mutational load and decreased fitness

20   due to lower efficiency of purifying selection at small effective population size. Genetic

21   rescue (GR) is a tool that is studied and deployed with the aim of increasing fitness of such

22   inbred populations. The success of GR is known to depend on certain factors that may vary

23   between different populations, such as their demographic history and distribution of

24   dominance effects of mutations. While we understand the effects of these factors on the

25   evolution of overall ancestry in the inbred population after GR, it is less clear what the effect

26   is on local adaptations and their genetic architecture. To this end, we conduct a population

27   genetic simulation study evaluating the effect of several different factors on the efficacy of

28   GR including trait complexity (Mendelian vs. polygenic), dominance effects, and

29 demographic history. We find that the effect on local adaptations depends highly on the

30 mutational load at the time of GR, which is shaped dynamically by interactions between

31 demographic history and dominance effects of deleterious variation. While local adaptations

32 are generally restored post-GR in the long run, in the short term they are often compromised

33 in the process of purging deleterious variation. We also show that while local adaptations are

34 almost always fully restored, the degree to which ancestral genetic variation comprising the

35 trait is replaced by donor variation can vary drastically, and is especially high for complex

36 traits. Our results provide considerations for practical GR and its effects on trait evolution.

37

38 **Keywords:** Genetic rescue; conservation genetics; local adaptations; mutational load;

39 dominance; demographic history; polygenic traits

40

1. Introduction

42   Genetic rescue (GR) is a strategy used in conservation biology to increase fitness of an

43 endangered inbred (recipient) population by introducing genetic variation from another

44 (donor) population. GR is accomplished by assisted migration of individuals from closely

45 related, healthy populations to the inbred imperiled population. This process naturally causes

46 the replacement of local genetic variation in the recipient population with that of the donor

47 population. Typically, only a small number of individuals are introduced in order to conserve

48 local genetic variation (Whiteley, Fitzpatrick, Funk & Tallmon, 2015).

49   The strategy has now been practiced on many highly inbred populations from different

50 taxa, including the Florida panther (Johnson et al., 2010), robins (Heber et al., 2012), guppies

51 (Fitzpatrick et al., 2016), wood rats (Smyser et al., 2013), and adders (Madsen et al., 1999). In

52 several cases, GR efficiently increased the absolute fitness of the inbred population and

53 reduced inbreeding depression (Frankham, 2015). A famous example is the introduction of

54 mountain lions from Texas of the sub-species *P. c. stanleyana* to the Florida *P. c. coryi*

55 population, for which the number of *P. c. coryi* increased three-fold after only five years, with

56 increased survival rates and a doubling of the heterozygosity (Johnson et al., 2010). A meta-

57   analysis provided evidence that the beneficial effect of GR can persist through the F3

58   generation (Frankham, 2016). These empirical tests suggest that GR is a powerful

59   conservation tool for increasing fitness in endangered inbred populations.

60   However, despite its promise, there is skepticism and caution towards the application of

61   GR due to concerns about outbreeding depression and genetic homogenization (Bell, *et al.*

62   2019). In the case of the Florida panther, an estimated genetic replacement of 41% has been

63   reported. In another case of the Isle Royale wolf, the immigration of one single male to Isle

64   Royale caused a genetic replacement of 56% to the local inbred population within two

65   generations (Adams et al. 2011). Hwang et al (2012) also reported a negative fitness effect

66   after practicing GR with two species that are genetically highly divergent due to outbreeding

67   depression.

68   Several different theoretical studies have been conducted to examine the expected

69   efficacy of GR (Hedrick, Hellsten & Grattapaglia, 2016; Harris, Zhang & Nielsen, 2019;

70   Tallmon et al., 2004; Frankham, et al., 2011). The dynamics of GR is complex, depending on,

71   among other factors, the amount of gene-flow, the demographic model (e.g. effective

72   population size), and the dominance coefficients of mutations. Harris et al (2019) showed that

73   with a higher amount of introgression, the relative fitness of the recipient population recovers

74   more quickly; however, this occurs at the cost of replacing an increasing proportion of the

75   recipient's ancestral genomes with those of the donor population. Demographic history of the

76   recipient and donor populations also determines the dynamics of GR. For example, small

77   effective population size (N_e) limits the efficacy of natural selection; thus, in most cases

78   admixture from a population with large N_e helps restore fitness (Harris et al., 2019). However,

79   several studies have shown that demography and dominance of deleterious mutations have

80   key interaction effects on the GR process (Harris et al., 2019; Kyriazis, Wayne & Lohmueller,

81   2019). For example, Kyriazis et al (2019) showed that fitness in populations with historically

82   low N_e can be more robust to severe bottlenecks than those with historically large N_e, as these

83   populations are less efficient at purging recessive deleterious mutations.

84   Previous studies suggest that the genetic replacement caused by GR can be controlled if

3

85   the amount of admixture is limited (Harris et al., 2019; Whiteley et al., 2015; Bell et al.,

86   2019). However, whether local adaptation plays a role in GR remains an open question.

87   Recently, Osmond & Coop (2019) investigated the population genetic signatures of selective

88   sweeps under evolutionary rescue, i.e. the adaptive response and recovery from reduced

89   absolute fitness due to environmental change. Also, Tomasini & Peischl (2019) investigated

90   the effect of local adaptations on evolutionary rescue. But whether GR would lead to the loss

91   of unique local adaptations, or whether local adaptations could affect the process of fitness

92   restoration by GR, remain largely unexplored.

93   Here, we explore how the addition of linked locally-adaptive variation affects the GR

94   process. Specifically, we explore the dynamics under GR of (1) a Mendelian trait, and (2) a

95   polygenic trait under stabilizing selection with a shift in the optimum. Our results illustrate

96   how the genetic architecture of adaptive traits evolve under GR, and how the dynamics of GR

97   depends on the joint effects of demographic models and genetic factors such as dominance.

98

99   **2. Materials and Methods**

100   We simulate under two demographic models from Harris, et al. (2019), as illustrated in

101   Figure 1. The simulations are conducted using SLiM (Haller & Messer, 2019). Model 1 (Fig.

102   1A) represents a population that undergoes a long-term bottleneck of 0.1 times the ancestral

103   population size ($N_e=10^4$), which last for 16,000 generations. This demographic history

104   represents a population that is inbred for a long period of time and is similarly to that

105   estimated for Neanderthals by Prufer *et al*. (2014). Neanderthals represent a good example of

106   a long-term inbred population where genomic analyses have discovered a substantial

107   accumulation of deleterious alleles (Prufer *et al.*, 2014). Model 2 (Fig. 1B) represents instead

108   a population with an extreme, short-lived bottleneck with $N_e=10$ that lasts for 20 generations,

109   which might be more representative of many currently endangered species. Prior to the time

110   of divergence, we conduct a burn-in phase of 44,000 generations. We simulate two modes of

111   adaptation: a Mendelian trait, with only one adaptive site contributing to the trait, and a

112   polygenic trait controlled by a large mutational target.

4

113   We simulate the Mendelian trait under two selection models: (1) a hard sweep, in which a

114   rare additive beneficial mutation occurs after the split of the population, and (2) a soft sweep

115   from a standing variant, in which an allele segregating neutrally leading up to the split is

116   picked at random, and its selection coefficient is then changed so that the allele is then

117   beneficial. Selection acts on the trait only after the split of two populations. For both models,

118   we have examined different selection coefficients, $s = 10^{-4}$, 10^{-3}, and 10^{-2} for the adaptive

119   mutation.

120   We simulate the polygenic trait under a model of stabilizing selection with Gaussian

121   fitness. To model the effects of local adaptation in the recipient population we allow the

122   phenotypic optimum in this deme to increase by some amount, immediately following the

123   divergence from the ancestral population. With V_S as the variance of the fitness function (not

124   to be confused with the variance in fitness among individuals), we simulated scenarios where

125   the inbred population's phenotypic optimum shifts by $\delta = 1, 2, 5$ immediately after the split,

126   while the phenotypic optimum remains 0 for the outbred population. We considered different

127   selection strengths by setting the variance of the fitness function to be $V_S = 3{,}000$ and $10{,}000$.

128   We assume genetic effects among loci are purely additive. Under this model, at equilibrium

129   (phenotypic mean equal to the optimum), alleles are under under-dominant selection with

130    $s = a^2/V_s$, where a is the effect of the allele, on the same scale on which the fitness

131   function is defined (Simons, $et\ al.$ 2018). In the transient phase after a large shift in the

132   optimum, selection is approximately additive with $s = a\delta/V_S$ (Hayward & Sella, 2019). In

133   order to ensure selection coefficients of causal SNPs are roughly $s \sim 10^{-4} - 10^{-3}$, in line

134   with current estimates that SNPs ascertained for complex traits in humans have been under

135   weak selection (Simons, et al. 2018), we draw the effects of causal alleles (a) from a standard

136   normal distribution (i.e. mean 0 and variance 1). See Table S1 for more details.

137   In addition to the adaptive mutations described above, we also allow for accumulation of

138   deleterious mutations assumed to be (1) additive (h=0.5), (2) partially recessive (h=0.1) and

139   (3) recessive (h=0), where h is the dominance coefficient. To specify a set of simulation

140   parameters realistic for mammals, we chose parameters estimated in humans for

141   recombination rates and distribution of fitness effects. We use the UCSC exon map from the

142   HG19 genome and the Distribution of Fitness Effect (DFE) on non-synonymous mutations

143   estimated by (Eyre-Walker, Woolfit, & Phelps, 2006), assuming a non-synonymous mutation

144   rate of 7×10^{-9} per bp/generation and log additive interactions among selected loci. A summary

145   of the simulations is provided in Supplementary Table S1.

146   For all simulations, we have recorded fitness in the inbred population relative to that of

147   the outbred population, the ancestry proportion in the inbred recovering population, the

148   varying allele frequency of the adaptive mutation in the Mendelian model, and the fluctuation

149   of mean phenotype in the stabilizing selection model.

150

151   **3. Results**

152   *3.1 Selection on Mendelian traits*

153   We simulated a Mendelian trait that is fixed for the derived (locally adaptive) allele in the

154   recipient population, and fixed for the ancestral allele in the donor population. We varied the

155   selection coefficient on the trait, the dominance coefficient of the linked deleterious variation,

156   the admixture proportion during GR, and the demographic model (Model 1 vs. Model 2, see

157   Fig. 1).

158   We investigated the effect of GR on fitness in the recipient population (i.e. hybrid fitness,

159   Fig. 2 A-C) as well as on ancestral genome proportion (Fig. 2 D-F). Fitness is measured by

160   taking the average of the fitness of offspring in the recipient population, and normalizing by

161   the same quantity for the donor population. The fitness calculated in generation T is the

162   fitness of parents (rather than offspring produced) in generation T. We found that, depending

163   on the demographic model and dominance of deleterious variation, GR has drastically

164   different success in terms of achieving rapid increase in hybrid fitness. For example, when

165   deleterious mutations are partially recessive, GR is successful but somewhat slow for Model 2

166   (Fig. 2E). In Model 1, under the same scenario, fitness is not fully recovered even after 1000

167   generations post admixture with 10% admixture from the donor population (Fig 2B). By

168   contrast, under a fully recessive load, fitness is restored extremely quickly under Model 2,

169   provided sufficient admixture (1%), whereas with the same level of admixture in Model 1,

170   fitness is not restored even in the long run (>1000 generations post admixture) (Fig 2C).

171   Generally, we find that the lower the recipient fitness before admixture, the higher the amount

172   of genomic replacement by the donor population in the long run (Fig. 2D-F). Furthermore, the

173   more successful the GR is at restoring fitness, the higher the amount of genomic replacement

174   in the long run (Fig. 2C,F). These conclusions are similar to those previously observed by

175   Harris *et al.* (2019).

176   We also considered how ancestry and fitness evolve jointly in the recipient population

177   (Fig. 3). Here, we show dynamics for a population under Model 2 with recessive deleterious

178   variation. We found that in the first generation after GR, native ancestry is either 0 or 100% in

179   the parents, where native ancestry is associated with much lower fitness (Fig. 3A). After one

180   generation of admixture, a large proportion of offspring were inbred-outbred crosses, despite

181   low admixture proportion (1%). Due to the large fitness advantage associated with outbred

182   ancestry, these crossed individuals enjoyed much higher fitness than not only the inbred

183   individuals, but also the non-crossed outbred individuals, because it is extremely rare for

184   these crosses to be homozygous for recessive deleterious variation (it would require a

185   recessive deleterious variant to segregate in both inbred and outbred populations since

186   divergence up to the admixture). In the following generations, as ancestry proportions range

187   between ~30-90%, there is a clear trend of lower native ancestry incurring increased hybrid

188   fitness (Fig. 3C,D)

189   A short term bottleneck (Model 2) does not increase or decrease the average number of

190   mutations an individual carries. However, it will allow recessive deleterious mutations of

191   strong effect, which were already segregating in the population, to increase in frequency and

192   potentially go to fixation (while others are lost). Models of recessive mutations allow for

193   much more standing variation of deleterious mutations, that potentially can increase in

194   frequency during the bottleneck, than models of additive mutations (e.g. Fig. 2A vs 2C). GR

195   is particularly effective in this case because the recipient population may have fixed strongly

196   deleterious recessive mutations that can be purged immediately after GR (Fig. 2C). In the case

7

197   of a constant low population size (Model 1), deleterious mutations (both in the recessive and

198   additive model) will accumulate and can slowly go to fixation if they have weak effects, but

199   one is unlikely to observe the same kind of strong effect of strongly deleterious recessive

200   mutations going to fixation as you would in models with recessive mutations and a bottleneck

201   (Fig. 2B-C).

202   Next, we looked at the dynamics of local adaptations under a Mendelian trait model (i.e.,

203   a single adaptive allele). We found that, in the short term (0-100 generations post-GR) the

204   adaptive allele decreases in frequency following the loss of ancestral DNA fractions (Fig. 4;

205   Fig. S1), which is the consequence of a selection-induced reduction in native ancestry after

206   the admixture (Fig. 2D-F). However, while the ancestral genome proportion continued to

207   decline slowly after 10 generations after GR (Fig. 2D-F), the adaptive allele generally

208   increased in frequency after 10-100 generations when enough recombination occurred to

209   break up linkage between the adaptive allele and the deleterious alleles. However, even for

210   very strong selection ($s = 0.01$), it took hundreds of generations for the adaptive allele to reach

211   high frequency in the population. In some extreme cases, with sufficiently high levels of

212   admixture (10%), GR under Model 2 actually caused the adaptive allele to be lost with high

213   probability after a total genetic replacement when the selection coefficient is sufficiently small

214   (≤ 0.001) (Fig. 4F).

215   We also examined the joint effects of dominance coefficients of linked deleterious

216   variation and demographic history on the efficacy of GR. Under both model I and II, we saw a

217   greater degree of genetic replacement (Figure 2D-F), leading to a greater reduction in the

218   frequency of the adaptive allele, as deleterious mutations become more recessive (Fig. 3 &

219   S1). For example, there was a smaller short-term reduction in allele frequency of the adaptive

220   allele under Model 2 (Fig. 4D-F, Fig. S1 D-F, relative to Model 1 [Fig. 4A-C, Fig. S1 A-C])

221   but a larger reduction for partially recessive/recessive deleterious variants (Fig. 4B,C,E,F, Fig.

222   S1 B,C,E,F), following the same pattern of the ancestral DNA proportion decline in those

223   scenarios (Fig 4. G-H). However, the locally adaptive locus itself had only a minor effect on

224   the recovery of relative fitness and reduction of ancestral DNA proportion of the recipient

225 population (Fig. 4, 5, S1, S2, S3). We considered that sweeps from standing variation may

226 have different patterns of linked deleterious variation around the adaptive allele; however,

227 when simulating under alternative selection models we found no difference between the hard

228 *vs* soft sweep models (see Fig. 4, S2, S3 vs Fig. S4, S5, S6).

229

230 *3.2 Polygenic adaptation*

231 We also simulated a polygenic trait under a model of stabilizing selection with a shift in

232 the optimum (Fig. 5-7). Here we varied the strength of stabilizing selection on the trait

233 (controlled by $\sqrt{V_S}$, the 'width' of the fitness function), the size of the shift in the local

234 optimum after population 2 diverges from population 1, $\delta = 0,1,2,5$, measured in units of

235 $\sqrt{V_S}$), dominance coefficient of deleterious mutations, admixture fraction during GR as well

236 as demographic model.

237 We examined two features of polygenic trait evolution: first, we evaluated the effect of

238 GR on the perturbation of the adaptive phenotype from its optimum (Fig. 5, Fig. S7); we

239 measure this by looking at the average distance of the population mean phenotype from the

240 optimum. We also considered the extent of replacement of ancestral variation causal for the

241 trait (Fig. 6); we measure this replacement by examining the relative proportion of genetic

242 variance of the trait due to ancestral variation *vs* donor variation introduced by GR.

243 We found that under Model 1, polygenic adaptations are not significantly affected by GR,

244 as the trait's evolution appears to follow the same trajectory regardless of admixture

245 proportions or dominance coefficients of the deleterious load (Fig. 5A-C). However, under

246 Model 2, we found that following rapid phenotypic drift from the optimum due to a severe

247 bottleneck (Fig. S7), polygenic adaptations subsequently follow dramatically different

248 trajectories depending on several factors (Fig. 5D-F): for example, GR allows the polygenic

249 adaptation to recover to its optimal value much more quickly than without GR (Fig. 5F); and

250 this effect is most pronounced under scenarios where there is fully recessive load (Fig. 5F),

251 although it is still significant under a partially recessive load (Fig. 5E).

252 We also explored how the genetic basis of the polygenic adaptation in the recipient

9

253 population is replaced by donor variation (Fig. 6). We quantify this using the proportion of the

254 genetic variance attributable to standing variation in the recipient population just before

255 admixture; genetic variance post-admixture is the sum of this quantity, plus genetic variance

256 attributable to standing variation in the donor population just before admixture, plus that of *de*

257 *novo* mutations occurring in the recipient population post-admixture (although this has

258 negligible contributions over short timescales). Generally, we find that the genetic basis is

259 quickly replaced due to GR, with >90% of the genetic variance being replaced with donor

260 variation when GR is most successful; for example, under Model 2, especially when the

261 deleterious load is recessive and the admixture fraction is high (Fig. 6A). Broadly, patterns of

262 genetic variance replacement are consistent with patterns of ancestry replacement (Fig. 6 *vs.*

263 Fig. 2D-F), with stronger replacement in situations where GR is more successful at recovering

264 fitness. However, details of the local adaptation do affect the dynamics of how the genetic

265 variance evolves; for example, when the optimal phenotype is more highly diverged in the

266 recipient *vs* donor population, the fraction of the genetic variance replaced by the donor

267 population is lower (Fig. 6B), because in this case donor individuals are more poorly adapted

268 to the environment of the recipient population, and thus GR is countervailed by this force.

269   Lastly, we directly compared hybrid fitness trajectories under the Mendelian *vs.*

270 polygenic trait models (Fig. 7). We found that, under the simulations models we considered,

271 varying parameters controlling the local adaptation does not have any appreciable effect on

272 hybrid fitness as an outcome of GR. In Fig. 7 we compare simulations of a Mendelian trait

273 under strong selection *vs.* a polygenic trait under strong stabilizing selection (see Methods).

274 The results are comparable both under Model 1 and Model 2 (Fig. 7A,B *vs* 7C,D) and under

275 various levels of dominance (Fig. 7).

276

277 **4. Discussion**

278   We have presented a population genetic simulation study that elucidates the dynamics of

279 local adaptation and genetic rescue (GR). We considered various models of the selection

280 strength and architecture of the adaptive trait, dominance of the mutational load, demography,

10

281 and admixture. The results of our simulations show that when a locally adaptive trait consists

282 of a single locus (e.g. a Mendelian trait), GR decreases the allele frequency in the short term.

283 Dominance of the linked deleterious variants and demographic history of the population

284 jointly determine the degree of its short-term loss while the strength of positive selection

285 determines the rate of trait recovery.

286 There are substantial differences in the evolutionary dynamics of the Mendelian trait and

287 the polygenic trait under GR. In simulations of a polygenic trait, the consequences of GR on

288 the trait is decided by both the loss of genetic materials as a whole and the distance between

289 the phenotype and its optimum before admixture. Generally speaking, it takes about 100

290 generations for a polygenic trait to return to its optimum in most cases, which is shorter than

291 that for a Mendelian trait under the same situation. Because polygenic traits have large

292 mutational targets, causal genetic variation that was previously exclusive to the donor

293 population is introduced to the inbred population via GR; this variation quickly replaces

294 native causal genetic variation, which is linked to many deleterious alleles. Thus, the

295 apparently higher efficiency with which the polygenic adaptation is restored comes at the cost

296 of long-term replacement by genetic variation from the donor population. We also showed

297 that the distance of the phenotypic optimum between the donor and the recipient population

298 has appreciable influence on how much genomic replacement is incurred by GR.

299 Our results demonstrate a marked difference between a long-term small effective

300 population size (Model 1) and a short-term severe bottlenecks (Model 2), with the latter

301 interacting strongly with the dominance of the deleterious mutation load. Our simulations

302 assume that, following GR/admixture, the effective population size of the recipient population

303 immediately recovers to the full size of the ancestral population. Future directions could

304 consider more gradual recoveries in the effective population size, possibly by using

305 evolutionary rescue models such as those discussed by Osmond & Coop (2019). Thus, our

306 models show GR operating at the upper limit of its efficiency, since the aforementioned

307 alternative models would have strictly lower effective population sizes in the short term

308 following admixture.

11

309   One caveat of our results is that our simulations do not assume epistasis and, therefore,

310   does not allow for the evolution of Dobzhansky-Muller incompatibilities (DMIs). However, in

311   the presence of DMIs, outbreeding depression may lead to limited genetic replacement or

312   even reduce the absolute fitness after GR.

313   Although our results suggest that locally adaptive traits, especially those that are

314   Mendelian or moderately polygenic, will be strongly affected by GR in the short term, but the

315   causal variant is generally retained and returns to fixation in the long run. While locally

316   adaptive polygenic traits are less susceptible to shifts due to GR, their underlying genetic

317   architecture is highly susceptible to long-term replacement by donor ancestry.

318

319   **References**

320   Adams, J. R., Vucetich, L. M., Hedrick, P. W., Peterson, R. O. & Vucetich, J. A. (2011).

321   Genomic sweep and potential genetic rescue during limiting environmental conditions in

322   an isolated wolf population. Proc. R. Soc. B.278:3336–3344.

323   Bell, D. A., Robinson, Z., Funk, W. C., Fitzpatrick, S. W., Allendorf, F. W., Tallmon, D. A., &

324   Whiteley, A. R. (2019). The Exciting Potential and Remaining Uncertainties of Genetic

325   Rescue. Trends in Ecology and Evolution, 34(12), 1070-1079.

326   Eyre-Walker, A., Woolfit, M., & Phelps, T. (2006). The distribution of fitness effects of new

327   deleterious amino acid mutations in humans. Genetics, 173(2), 891–900.

328   Fitzpatrick, S. W., Gerberich, J. C., Angeloni, L. M., Bailey, L. L., Broder, E. D., Torres-

329   Dowdall, J., Handelsman, C. A., López-Sepulcre, A., Reznick, D. N., Ghalambor, C. K.,

330   & Chris Funk, W. (2016). Gene flow from an adaptively divergent source causes rescue

331   through genetic and demographic factors in two wild populations of Trinidadian guppies.

332   Evolutionary applications, 9(7), 879–891.

333   Frankham, R., Ballou, J.D., Eldridge, M.D.B., Lacy, R.C., Ralls, K., Dudash, M.R. & Fenster,

334   C.B. (2011), Predicting the Probability of Outbreeding Depression. Conservation

335   Biology, 25: 465-475.

336   Frankham, R. (2015). Genetic rescue of small inbred populations: meta-analysis reveals large

337   and consistent benefits of gene flow. Molecular Ecology, 24(11), 2610-2618.

338   Frankham, R. (2016). Genetic rescue benefits persist to at least the F3 generation, based on a

339   meta-analysis. Biol. Conserv., 195, 33-36

340   Haller, B. C., & Messer, P. W. (2019). SLiM 3: Forward Genetic Simulations Beyond the

341   Wright–Fisher Model. Molecular Biology and Evolution, 36(3), 632-637.

342   Harris, K., Zhang, Y., & Nielsen, R. (2019). Genetic rescue and the maintenance of native

343   ancestry. Conservation Genetics, 20(1), 59-64.

344   Hayward, L. K., & Sella, G. (2019). Polygenic adaptation after a sudden change in

345   environment. bioRxiv,

346   Heber, S., Varsani, A., Kuhn, S., Girg, A., Kempenaers, B., & Briskie, J. (2012). The genetic

347   rescue of two bottlenecked South Island robin populations using translocations of inbred

348   donors. Proceedings. Biological sciences, 280(1752), 20122228.

349   Hedrick, P. W., & Garciadorado, A. (2016). Understanding Inbreeding Depression, Purging,

350   and Genetic Rescue. Trends in Ecology and Evolution, 31(12), 940-952.

351   Hedrick, P. W., Hellsten, U., & Grattapaglia, D. (2016). Examining the cause of high

352   inbreeding depression: analysis of whole‐genome sequence data in 28 selfed progeny

353   of Eucalyptus grandis. New Phytologist, 209(2), 600-611.

354   Hedrick, P. W., Robinson, J. A., Peterson, R. O. & Vucetich, J. A. (2019) Genetics and

355   extinction and the example of Isle Royale wolves. Anim. Conserv., 22(3), 302-309

356   Hwang, A. S., Northrup, S. L., Peterson, D. L., Kim, Y., & Edmands, S. (2012). Long-term

357   experimental hybrid swarms between nearly incompatible Tigriopus californicus

358   populations: persistent fitness problems and assimilation by the superior population.

359   Conservation Genetics, 13(2), 567-579.

360   Johnson, W. E., Onorato, D. P., Roelke, M. E., Land, E. D., Cunningham, M. W., Belden, R.

361   C., ... & Obrien, S. J. (2010). Genetic Restoration of the Florida Panther. Science,

362   329(5999), 1641-1645.

363   Kyriazis, C. C., Wayne, R. K., & Lohmueller, K. E. (2019). High genetic diversity can

364   contribute to extinction in small populations. bioRxiv.

365 Madsen, T., Shine, R., Olsson, M. et al. (1999). Restoration of an inbred adder population.
366   Nature 402, 34–35.

367 Osmond, M. M., & Coop, G. (2019). Genetic signatures of evolutionary rescue by a selective
368   sweep. bioRxiv.

369 Prufer, K., Racimo, F., Patterson, N., Jay, F., Sankararaman, S., Sawyer, S., ... & Paabo, S.
370   (2014). The complete genome sequence of a Neanderthal from the Altai Mountains.
371   Nature, 505(7481), 43-49.

372 Simons, Y. B., Bullaughey, K., Hudson, R. R., & Sella, G. (2018). A population genetic
373   interpretation of GWAS findings for human quantitative traits. *PLoS biology*, *16*(3),
374   e2002985.

375 Smyser, T. J., Johnson, S. A., Page, L. K., Hudson, C. M., & Rhodes, E. J. (2013). Use of
376   experimental translocations of Allegheny woodrat to decipher causal agents of decline..
377   Conservation Biology, 27(4), 752-762.

378 Tallmon, D. A., Luikart, G., & Waples, R. S. (2004). The alluring simplicity and complex
379   reality of genetic rescue. Trends in Ecology and Evolution, 19(9), 489-496.

380 Tomasini, M., & Peischl, S. (2019). When does gene flow facilitate evolutionary rescue.
381   bioRxiv.

382 Whiteley, A. R., Fitzpatrick, S. W., Funk , W. C. & Tallmon, D. A. (2015) Genetic rescue to
383   the rescue. Trends in Ecology & Evolution 30: 42-49.

384
385 **Data accessibility**

386

387 Scripts are available on GitHub at https://github.com/YulinZhang9806/GR_adaptation_scripts.

388

389 **Authors contribution**

390

394
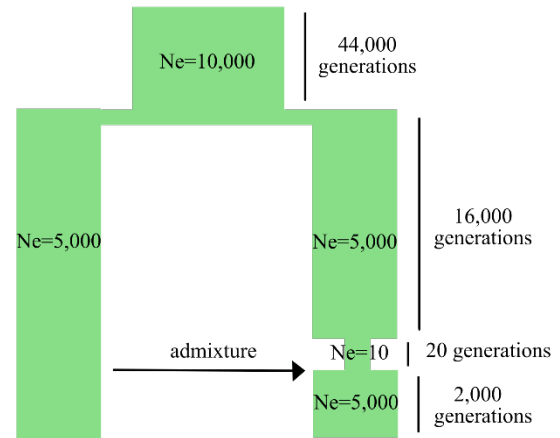
A. Model 1
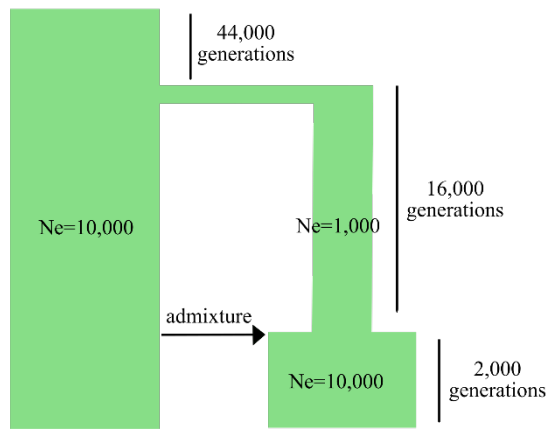
B. Model 2

Figure 1. Two demographic models used for simulations. Time runs from top to bottom. Admixture happens at the generation right after the population size increases and lasts for only one generation. Population size changes are assumed to be discrete as depicted in the figure. Samples are taken from the inbred population on the right (p2) after the admixture up to 2,000 generations.
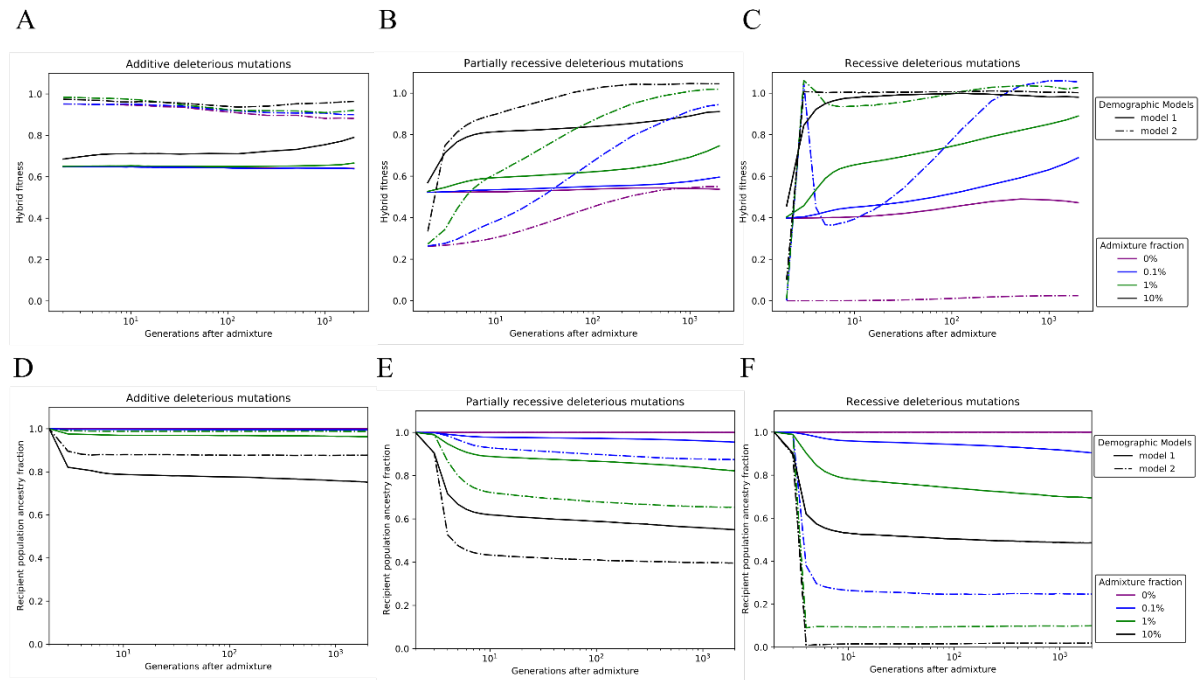
Figure 2. (A-C) Hybrid fitness change of the inbred population after admixture and (D-F) Recipient population ancestral genome fraction changes after GR with a Mendelian adaptive trait, under hard sweep selection model and demographic Model 1 (solid lines) and demographic Model 2 (dashed lines). The adaptive mutation is additive (dominance coefficient h=0.5) while selection coefficient is set differently (shown with different line styles in A-F). Deleterious mutations are assumed additive (h=0.5) in A, D, partially recessive (h=0.1) in B,E and recessive (h=0) in C,F.
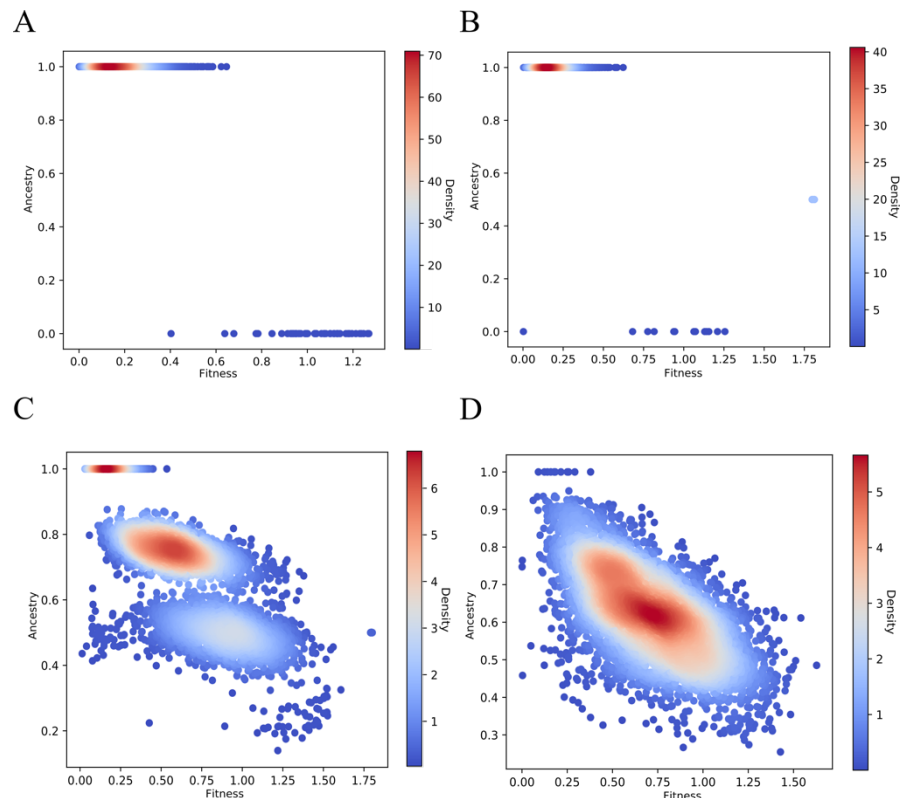
Figure 3. Relation between individual fitness and its ancestral genome proportion under demographic Model 2, with recessive deleterious mutations and admixture fraction of 1%. Each dot represents an individual, depicting relation between ancestry proportion and relative fitness (to the mean fitness of the outbred population) of each individual in the inbred recipient population. Figure A shows the population before mating with outbred individuals. Figure B indicates the first generation after admixture (e.g. F1), while figure C represents the second generation (e.g. F2) and figure D shows the third generation (e.g. F3).
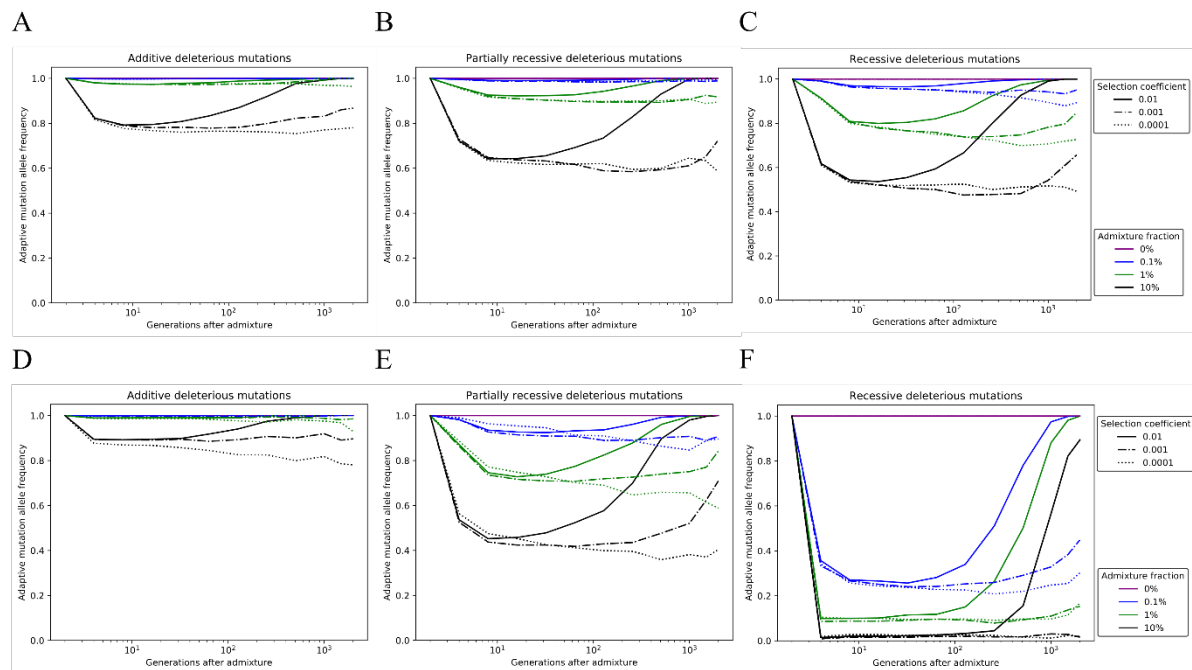
Figure 4. Allele frequency changes after admixture for a Mendelian trait under hard sweep selection model and (A-C) demographic Model 1 (D-F) demographic Model 2. The adaptive mutation is additive (dominance coefficient h=0.5) while selection coefficient is set differently (shown with different line styles). Deleterious mutations are assumed additive (h=0.5) in A, D, partially recessive (h=0.1) in figure B,E and recessive (h=0) in C,F.
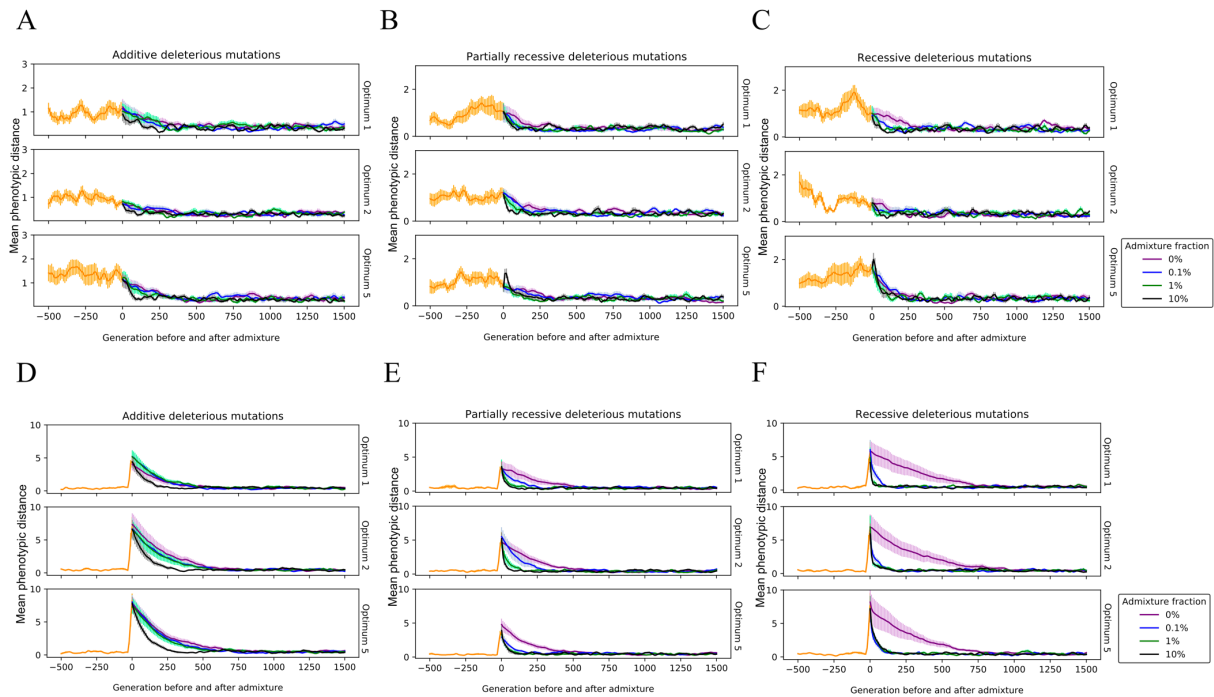
Figure 5. Mean phenotype distance from optimum over time. (A-C) Simulations under Model 1, (D-F) simulations under Model 2. Shaded bars signify 95% confidence intervals for the mean phenotypic distance.
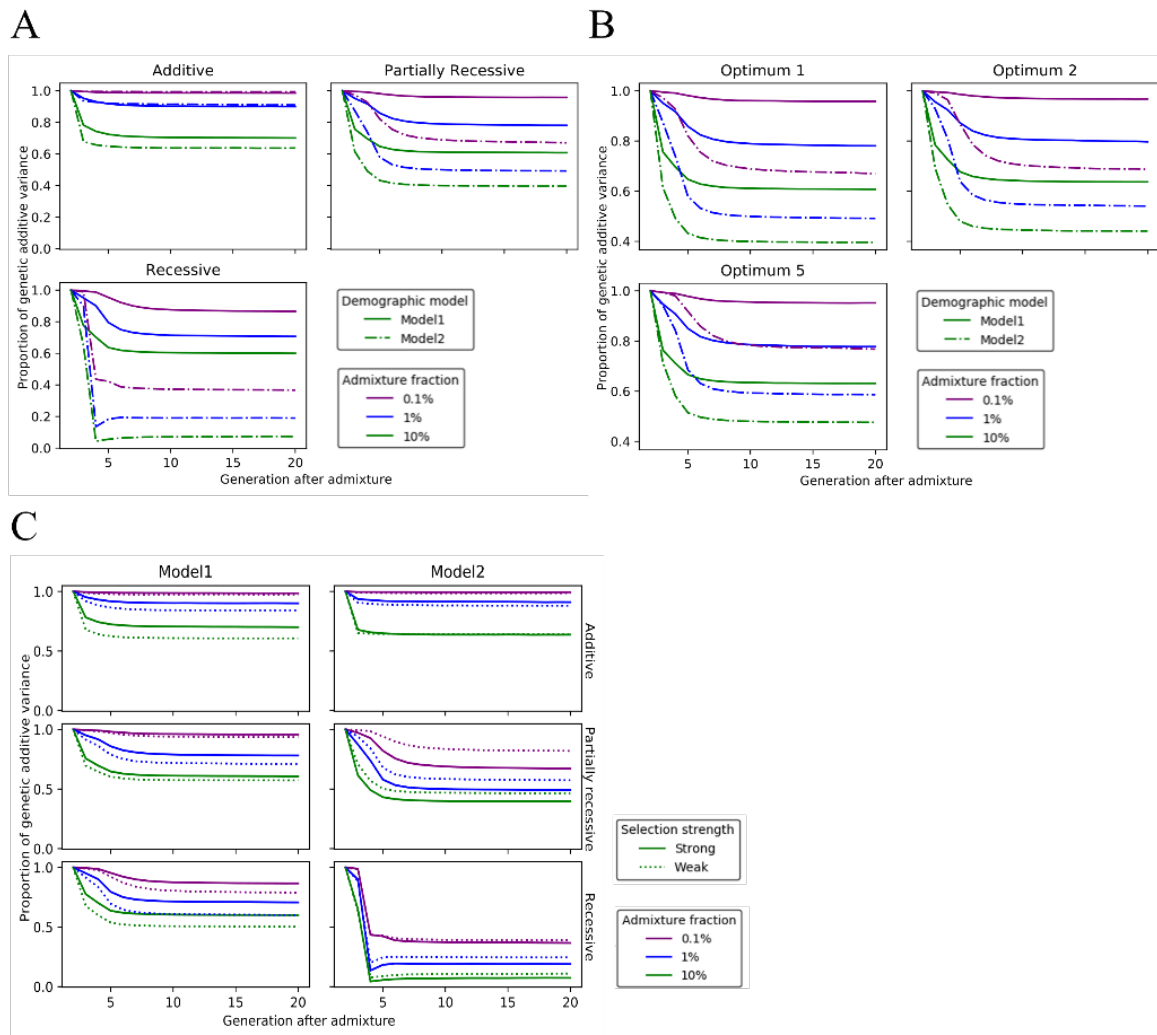
Figure 6. Proportion of genetic additive variance of a polygenic adaptation, recording mutations that originate from the recipient population for 20 generations after GR. (A) Scenarios under strong selection, with optimum of 1 for the recipient population and different dominance coefficients for deleterious mutations. (B) Scenarios under strong selection, with partially recessive deleterious mutations and different optimum for the recipient population. (C) Scenarios with optimum equals 1 and different selection strength for the adaptive trait. Each line represents the proportion of genetic additive variance contributed by variants, which compose the trait, from the ancestral genome of inbred population. Here, genetic additive variance is calculated as $G = \sum_{l \in SNPs} 2a_l^2 p_l(1 - p_l)$, where a_l represents the effect of SNP l, and p_l its frequency.
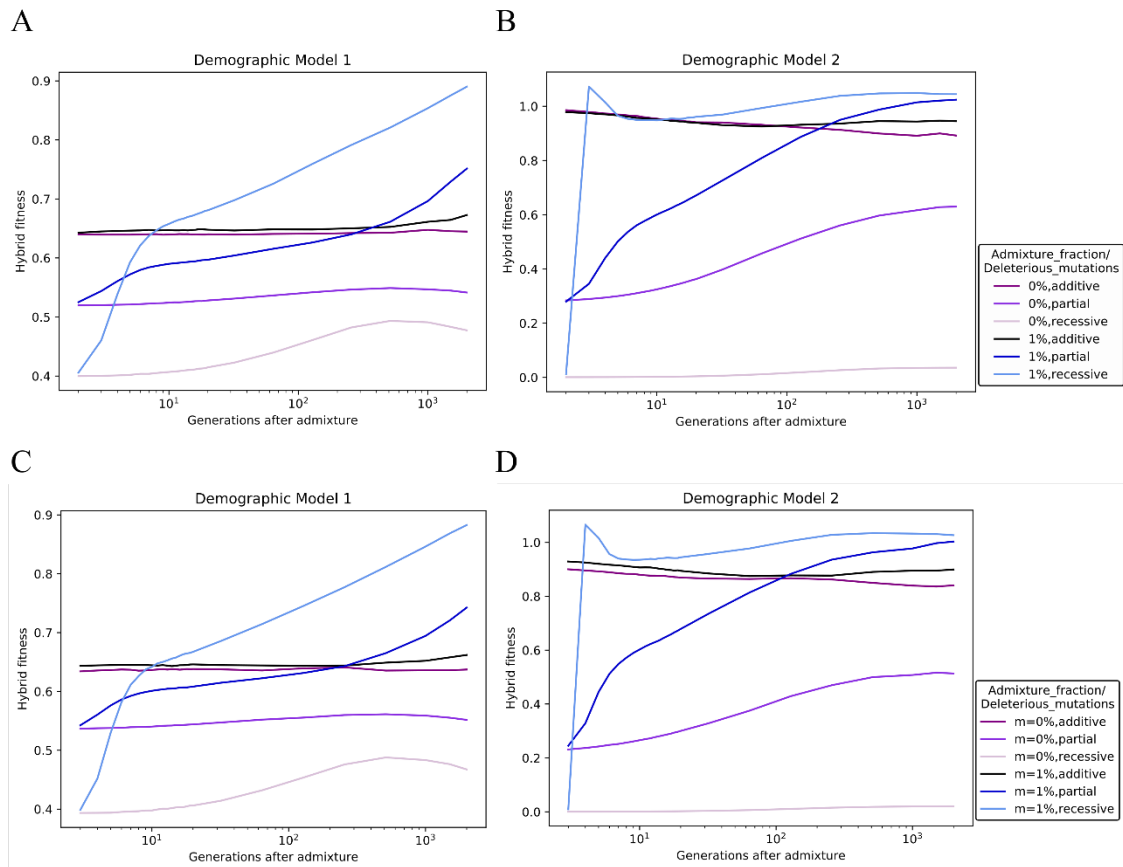
Figure 7. Hybrid fitness changes of the inbred population after admixture with (A-B) a Mendelian adaptive trait, under hard sweep selection model and (C-D) a polygenic trait under stabilizing selection with strong selection. Figure A and C are results of demographic Model 1 while B and D are that of demographic Model 2. Lines of different colors are indicating scenarios with different admixture fraction and dominance (of deleterious mutations).